External Lightning Protection and Grounding in Large-Scale Photovoltaic Applications

Charalambos A. Charalambous, *Member, IEEE*, Nikolaos D. Kokkinos, and Nikolas Christofides

***Abstract*—The development of large-scale photovoltaic (PV) plants in rural areas is constantly increasing. However, the knowledge of performing and installing lightning and surge protection in large-scale PV plants is still premature. The main objective of this paper is to provide a method for assessing the external lightning protection and earthing designs that may be installed in large-scale solar applications. Consequently, the method and models presented in this paper may assist engineers to perform a comparison between the use of isolated and nonisolated lightning protection systems, and second to select suitable surge protection equipment.**

***Index Terms*—Earthing, large-scale PV plants, lightning protection.**

I. Introduction

THE installation of an efficient lightning protection system (L.P.S) for large-scale photovoltaic (PV) plants is important by virtue of its preventing nature. Primarily, this importance lies in preventing any physical damage to structures as well as life hazards.

Furthermore, it should be borne in mind that the capital investments for large-scale PV plants are significant and the investors should choose to adopt an appropriate L.P.S for their systems. In fact, the cost of installing an L.P.S may be proved insignificant when compared to the revenue losses incurred due to failures or damages resulting from a lightning strike. One should also consider the practical difficulties associated with the repairs or component replacements.

Nevertheless, the knowledge of performing and installing lightning and surge protection in large and extended PV plants with long cabling loops is, in most of the cases, still precipitous. It is worth noting that the recent development of the new CENELEC document of TS 50539-12: 2009 by WG1 of CLC TC37 A [1] only describes the application principles for surge protection in PV installations on roofs of domestic structures.

Moreover, a thorough literature survey reveals that there is still very little information published regarding the design of lightning and surge protection for large-scale solar applications. In particular, the work described in [2] comprehensively covers the related scientific background of any previous work [3], [4] and further emphasizes the lack of 1) specific field experience and 2) a universal standard method to address the problems. To this extent, the current practice, for protecting small-scale PV installations from lightning surges, rests with adopting (partly) protective measures described in standards for conventional low-voltage power distribution systems [5]–[7]. On a relevant note, the work in [8] describes a scaled down laboratory test to investigate the performance of nonisolated and isolated external L.P.S designs in controlling the induced voltages across the dc cable loop of the string due to a lightning strike.

The simulation models formulated in this paper are based on topologically accurate 3-D designs and on other material particulars found in real-life applications. It should be noted that the topologically accurate models include the earthing system arrangement and the metallic PV supporting frames simulated under different scenarios. These models were designed and processed within a commercial software platform utilizing methods described in [9]. The models can be used to assess the design options and the lightning current distribution across large-scale PV parks. Thus, the main objective of this paper is to assess the external lightning protection and earthing design options that are installed in these applications. On a final note, this paper does not account for any induced voltages and currents into the PV arrays that are subject to related lightning channels and flows of the return strokes.

II. Fundamental Design Principles of External L.P.S and Earthing Systems for Large-Scale PV Systems

The design options considered in lightning protection endeavors should be subject to an appropriate risk assessment. The risk assessment may be performed according to IEC-62305-2 [10], which provides a procedure for the evaluation of risk (based on different types of loss) to a structure, due to lightning flashes to earth. For example, in large-scale PV applications, the economic losses may be the dominating factor that determines which type of surge protection should be employed. It is emphasized, however, that this paper takes a step forward and focuses on the design principles of an external L.P.S and earthing systems of the large-scale PV systems. These protection systems are assumed to be the product of appropriate risk assessments.

The L.P.S first embraces the air termination system, which intercepts between the lightning and the physical parts of the protected structure. Second, it embraces the down conductors which discharge the lightning current to an earth termination

Manuscript received May 24, 2013; revised June 25, 2013 and August 22, 2013; accepted August 26, 2013.

C. A. Charalambous is with the Department of Electrical and Computer Engineering, University of Cyprus, Nicosia 1687, Cyprus (e-mail: cchara@ucy.ac.cy).

N. D. Kokkinos is with ELEMKO SA, 144 52 Athens, Greece (e-mail: n.kokkinos@elemko.gr).

N. Christofides is with the Department of Electrical Engineering, Frederick University, Nicosia 1036, Cyprus (e-mail: n.christofides@frederick.ac.cy).

Color versions of one or more of the figures in this paper are available online at http://ieeexplore.ieee.org.

Digital Object Identifier 10.1109/TEMC.2013.2280027

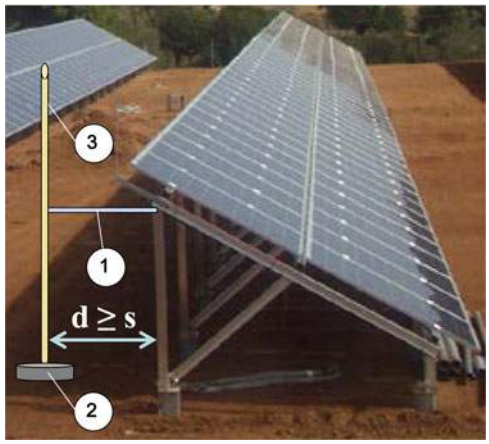

Fig. 1. Isolated L.P.S in PV applications. (1) Isolating support. (2) Concrete block base. (3) Air termination rod.

system. The earth termination system discharges the lightning current into the general mass of the earth.

A. Design Principles of External L.P.S

The main design methods of air termination systems in solar applications are the protection angle or the rolling sphere method. The protection angle method assumes a number of air termination rods with sufficient height, installed along the entire length of the PV supporting infrastructure. These will offer a protection angle which fulfills the required protection set by the L.P.S class [5]. In contrast, when the rolling sphere method is applied, the positioning of the air termination system should ensure that no point of the supporting infrastructure is in contact with a sphere of radius R. To this extent, the external L.P.S can be designed to be isolated or nonisolated from the PV application. The isolated L.P.S is commonly used in cases of high risk damage from the lightning current (should this pass through the metallic installations that are directly connected to the L.P.S). An isolated L.P.S consists of a free standing mast (embracing the air termination rod and the down conductor), which stands away from the PV metallic support frame at a distance d (see Fig. 1).

The separation distance d should always be greater or equal to a minimum separation distance s calculated as follows:

$$s = \frac{k_i}{k_m} \times k_c \times l \tag{1}$$

where k_i is a constant that depends on the selected class of the L.P.S, k_m is a constant that depends on the electrical insulation material, k_c is a constant that depends on the (partial) lightning current flowing in the air termination and the down conductor, and l is the length, in meters, along the air termination and the down conductor [6]. Distance l spans from the top level of the PV supporting infrastructure to the nearest equipotential bonding point or the earth termination system (i.e., ground level).

An example of a nonisolated L.P.S is shown in Fig. 2. This is directly installed on the PV frame provided that the metallic façade/frame can be utilized as a natural component of the L.P.S. However, in such a case, there are certain requirements that need

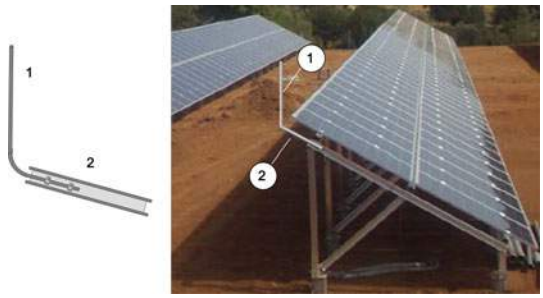

Fig. 2. Nonisolated L.P.S in PV applications. (1) Aluminum air termination rod. (2) Connection clamp.

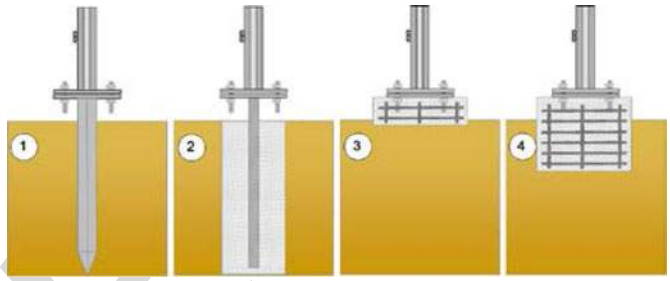

Fig. 3. Type of foundation for an earthing system of the open-field PV applications.

TABLE I
TYPE OF FOUNDATION AND MATERIALS FOR AN EARTHING SYSTEM

	Type of Foundation	Material for Earthing System Driven into the Soil
1	Galvanized steel directly buried into the soil	Galvanized steel, Stainless steel
2	Steel profile embedded in concrete	Copper coated steel, Copper, Stainless steel
3	Reinforced concrete block placed above ground level	Galvanized steel, Copper coated steel, Copper, Stainless steel
4	Reinforced concrete foundation into the soil	Copper coated steel, Copper, Stainless steel
Note 1: Copper Conductor may be tinned; Note 2: Aluminum not allowed to be buried into the soil		

to be fulfilled as per the clause 5.3.4 of IEC/EN 62305-3. These requirements are summarized as follows: 1) the dimensions of the metallic façade should conform the requirements of EN 50164-1&2 [11], [12] and future IEC 62561-2, and 2) the connections along the metallic façade length shall be secure by such means as brazing, welding, clamping, crimping, screwing, or bolding.

B. Design Principles of Earthing Systems

A primary objective in designing the earthing system of a large-scale PV application is to maintain a balance between the installation cost as well as the efficiency and lifetime of the system. Consequently, an important parameter that the designer should take into account when selecting the earth electrode material is the foundation type employed in PV façade framework. That is to avoid the galvanic corrosion between metals of dissimilar nature. Thus, all the materials used (i.e., earth rods, bonding conductors, metallic façade, clamps) should be homogeneous. Fig. 3 illustrates the most common types of PV framework foundations and Table I tabulates their description and the associated material characteristics of the earthing system driven into the

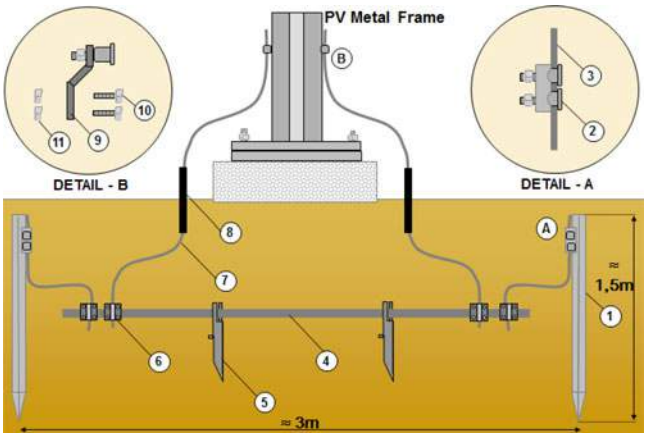

Fig. 4. Application example of type A earth electrode of hot dip galvanized material in combination with dip driven galvanized steel profiles or reinforced concrete blocks.

TABLE II
DESCRIPTION OF THE ELEMENTS ON TYPE A APPLICATION EXAMPLE

	Description
1	Hot dip galvanized steel (St/tZn) earth rod cross profile with zinc coating of 500 g/m² (~70 μm coating thickness), 1.5 m long tested as per EN 50164 -2
2	Hot dip galvanized steel double bonding clamp between St/Zn 10 mm round conductor and St/Zn cross profile earth rod tested as per EN 50164 1 (Type H 100 kA)
3	Hot dip galvanized steel round conductor 10 mm diameter with zinc coating of 50 μm long tested as per EN 50164 -2
4	Hot dip galvanized steel strip conductor with dimensions 30mm x 3mm zinc coating of 500 g/m² (~70 μm coating thickness), tested as per EN 50164 -2
5	Hot dip galvanized steel strip conductor fastener for vertical installation of the strip conductor.
6	Hot dip galvanized steel clamp St/tZn 10mm round conductor and St/tZn 30mm wide strip conductor tested as per EN 50164 -1 (Type II – 100kA)
7	Hot dip galvanized steel round conductor 10mm diameter with zinc coating of 50 μm tested as per EN 50164-2.
8	Corrosion protection PVC insulation tape
9	Aluminum (Al) end clamp between metallic (St/tZn or Al) surface and St/tZn 10 mm round conductor tested as per EN 50164 – 1 (Type H -100 kA)
10, 11	2 x stainless steel or hot dip galvanized (St/tZn) M8 screw and nut

soil, to avoid galvanic corrosion, thus extending the life time of the installation.

Furthermore, the large area that the solar field applications occupy suggests the combined use of type A and type B earthing systems [16]. The most common type A electrodes, utilized in large-scale solar applications, are the earth rods which are vertically installed into the soil. The field experience suggests that at least two rods should be used per down conductor as illustrated in Fig. 4 having a minimum length of 1.5 m. Furthermore, it is also important to maintain a distance between the earth rods installed $\sim$2 times their length. Table II tabulates the elements and material characteristics of Fig. 4.

For type B earth electrodes, the most common shape used is the strip conductor. The use of type B electrodes ensures the equipotential bonding of all PV metal frameworks. Fig. 5 illustrates an application of a type B earth electrode in an open-field solar application. A common mesh size spans on a $20m \times 20m$ basis, although wider mesh sizes such as $40m \times 40m$ may also be utilized when combined with type A electrodes.

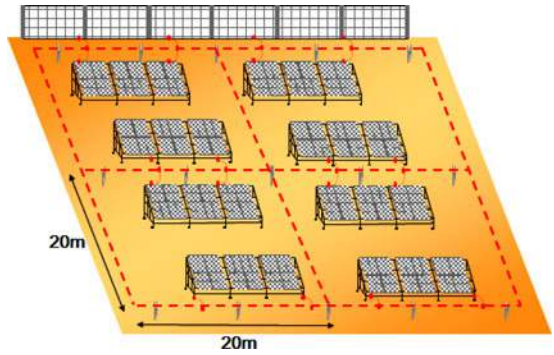

Fig. 5. Application of type B earth electrode in an open-field PV application.

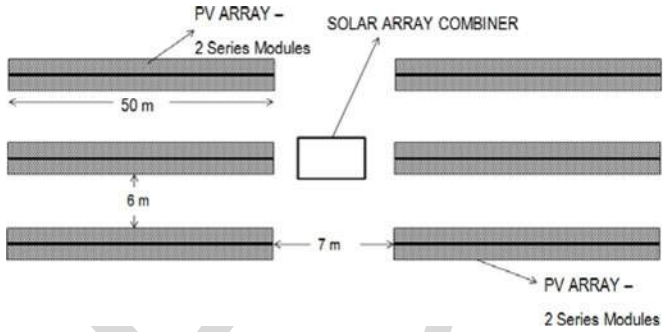

Fig. 6. Topology of the 150-kWp PV system.

III. DESCRIPTION OF THE SIMULATION MODELS

The real-scale simulation models were formulated within a commercially available software by following an assessment of the infrastructure elements considered to contribute to the lightning performance of both isolated and nonisolated L.P.S installed on large-scale solar applications. The software employs a Cartesian coordinate system with three coordinates (x, y, z), thus allowing the formation of topologically accurate simulation models, through the use of conductors. The arrangement of conductors is specified by virtue of its energization method, the magnitude of the energization, its material coating characteristics, and the coordinates of each conductor along with its radii and number of specified segments. The conductors segments can be subsequently associated with various energization types (potentials, current injections, and current flows) [9], [13].

A. Description of the System

The system considered consists of 600 250 Wp modules, directly linked to the MV network, with a nominal output power of 150 kWp, occupying an area of 1605 m^2. Six similar structures (arrays) of fixed inclination are considered and each structure holds up to 100 modules as is shown in Fig. 6. The length of each PV array is 50 m and two rows of PV modules are assumed to be installed on each structure.

Furthermore, Fig. 7 illustrates an earthing design example when a non isolated L.P.S is installed in the solar field applications. It specifically shows two rows of PV arrays (6 m away) that are connected to a common earth electrode via the metallic framework.

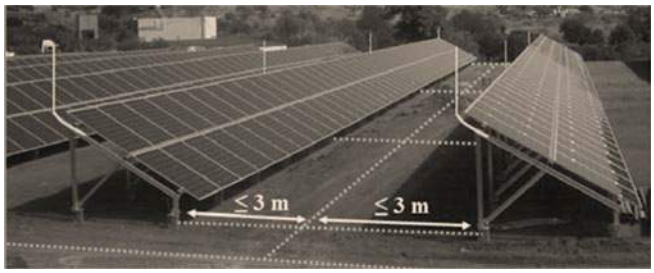

Fig. 7. Example of nonisolated L.P.S and earthing design for large-scale solar field applications.

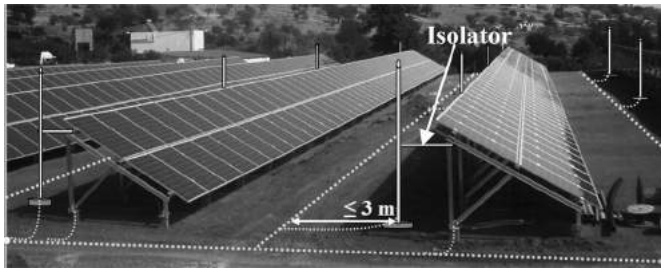

Fig. 8. Example of isolated L.P.S and earthing design for large-scale solar field applications.

Alternatively, Fig. 8 illustrates an application of an isolated L.P.S and its associated earthing design. It shows that the isolated air termination rods are connected directly to a circumference earth electrode; thus, each row of air termination rods have its own earth electrode. It should be noted that in the case of isolated L.P.S, the earthing system should be designed in such a way to prohibit the circulation of any lightning current through the PV frame.

B. Description of the Simulation Model

Two real-scale simulation models are developed within the software's modules for the 150 kWp PV fixed inclination system of Fig. 6. Following the dimensions given in Fig. 6 and an external L.P.S design similar to Fig. 7, the ideal computer model formulated, for a nonisolated external lightning protection application, is illustrated in side view in Fig. 9.

Fig. 10 also illustrates the design dimensions considered for the PV structural base modeled in the simulation model—to facilitate the fixed inclination of the array structures.

Table III tabulates the further particulars of the numbered items of the conductive elements employed in the computer model (see Fig. 9).

Moreover, (to limit the overall number of conductors used in the model), only one array/string combiner, that may accommodate 150 250 Wp modules, is modeled. As is shown in Fig. 9, a total of six strings (S_1–S_6) lead to the inverter and each string consists of 25 modules in series. In fact, the six strings terminate into the array/string combiner box and from then on to the inverter. The latter simplifies the dc wiring considerably as no overlapping will be necessary between structures and the wiring is kept at its minimum.

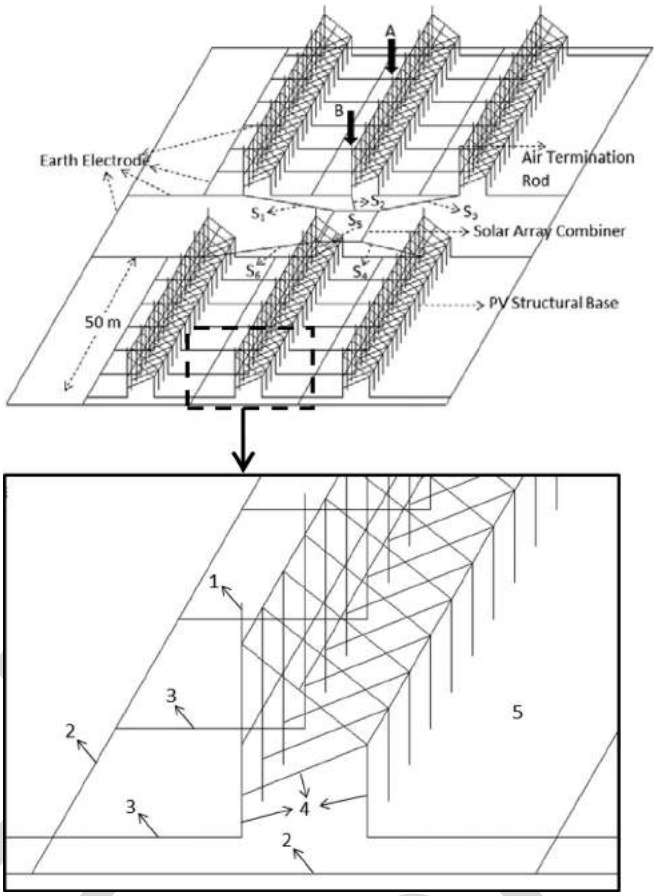

Fig. 9. Real-scale simulation model for a 150-kW solar park—with nonisolated L.P.S.

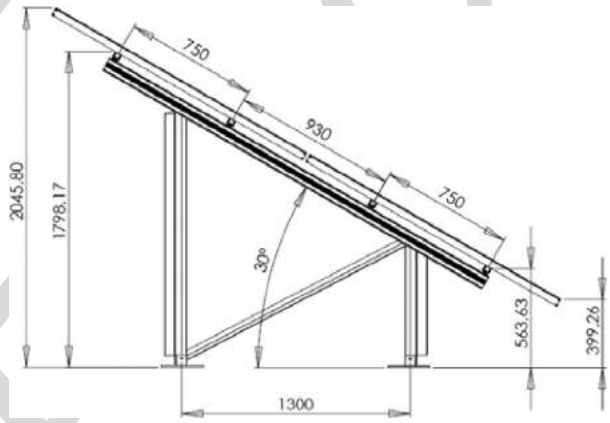

Fig. 10. Design dimensions (mm) of the PV structural base —side view.

Fig. 11 illustrates the ideal simulation model formulated for the same PV application and design characteristics shown in Fig. 6 having, however, an isolated external L.P.S design as illustrated in Fig. 8. In this model (see Fig. 11), the lightning rod (item 1_A) is isolated from the PV structural base. More specifically, this is an aluminum air termination rod, Φ16 mm, 3 m long, located 0.5 m away from the structural base, and is attached to a circumference earth electrode as shown in Fig. 11. The further particulars of the numbered items of the conductive

TABLE III
DESCRIPTION OF THE CONDUCTIVE ELEMENTS OF THE SIMULATION MODEL

Numbered Items	Further Particulars
Attached Lightning Rod (Item 1)	Aluminium air termination rod, Φ16mm, 1m long, attached on the PV support structure. Designed as per Class I L.P.S [5] Number of Lightning Rods*: 7 Spacing*: ~7m *Evaluated as per IEC 62305-3 [16] (rolling sphere method)
Earth Electrodes (Items 2 & 3)	Earth electrodes are made of copper conductors (CSA 50mm^2) buried into soil at a depth of 0.5m. The structural PV base is bonded (item 3) to the circumference earth electrode (item 2) to ensure an equipotential continuity.
Structural Base (Item 4)	Geometrically accurate aluminium support PV structure as per the dimensions given in Fig 10. Each metallic component of the base is approximated by 10mm radius aluminium conductors. The vertical conductors (legs) of the structure are driven to a depth of 1.5m into the earth.
Soil (Item 5)	The soil resistivity is assumed to be 100 Ω.m.

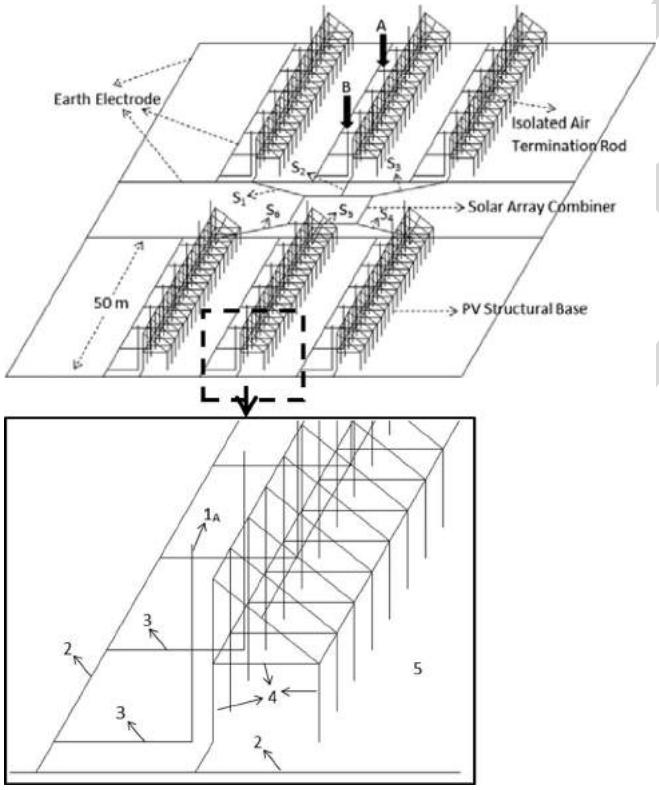

Fig. 11. Real-scale simulation model for a 150-kW solar park—with isolated L.P.S.

elements employed in this computer model are the same as those tabulated in Table III.

Finally, two possible locations (A or B) for lightning current injections are assumed in this paper, for both the simulation models shown in Figs. 9 and 11. These locations are arbitrary chosen, however, location B may be considered as a worst case scenario as it is closer to the array/string combiner box. It is noted that the model is able to account for any other lightning injection location specified by the user. The lightning surge currents considered in this paper are defined by double exponential type functions. A lightning surge current *I(t),* can be injected at the specified location (A or B) as illustrated by Figs. 9 and 11. The current is classified as 150 kA 10/350 μs, to account for a lightning protection class (L.P.C) II as per IEC 62305-1. The corresponding double exponential function considered is given as follows:

$$I(t) = 153664 \times 10^3 \cdot \left[e^{-a \cdot t} - e^{-\beta \cdot t}\right] \tag{2}$$

where $\alpha = 2049$ and $\beta = 563758$.

On a final note, the 150-kWp PV plant, considered previously is assumed to be directly connected to the LV or the MV grid via a transformer (e.g., installed on wooden poles). It should be noted that for PV plants of higher power level, a high-voltage substation may be required [14]. However, the lack of specific standards calls for further research to justify different earthing design methods that balance cost and safety. For example, a 4-MW PV park may occupy a field area that equals to 90000 m^2. A uniform mesh size grid (as used in ac substations) across the field may be prohibitively expensive at this scale; however, safety should not be compromised.

IV. SIMULATION RESULTS AND ANALYSIS

The ultimate objective of the simulations is to assess the lightning current distribution across a large-scale PV park, under the two different external L.P.S design options (isolated or non-isolated). The simulations are carried out using the two models illustrated in Figs. 9 and 11, respectively. This exercise is particularly important as it may facilitate an appropriate specification (discharge current capability) of the surge arrester devices entitled to protect the inverter, based on the topology and type of protection of each individual solar application.

A. Reference to Computational Methods

The software computes the current distribution for the networks modeled (see Figs. 9 and 11) consisting both the aerial and buried conductors excited at selected frequencies, determined by the type of lightning current considered. The details of the evaluation method are given in [9] and [13].

The time-domain responses are obtained as follows. The double exponential 150-kA function (2) is decomposed into its frequency spectrum, by a forward fast Fourier transform. For the 150-kA double exponential function considered (2), computations are carried out for selected frequencies ranging from 0–1 MHz. At selected frequencies, the electromagnetic fields are calculated at various observation points, on the conductor network, to obtain the frequency spectrum of the electromagnetic fields. The time-domain transient current profiles, through each conductor (or observation point) of the system, are subsequently calculated by appropriately superimposing the frequency domain responses obtained.

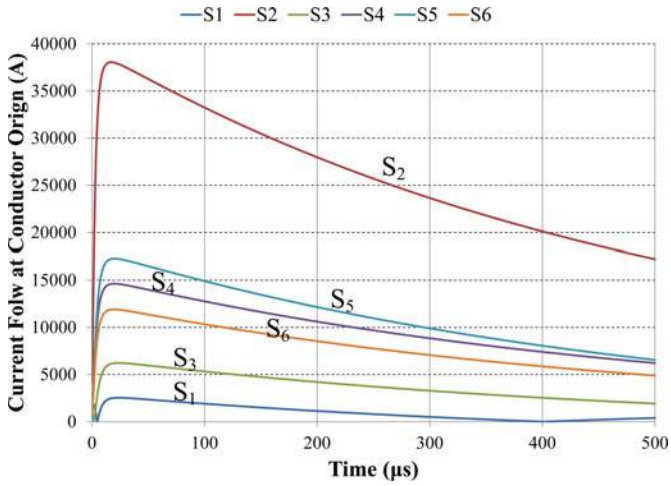

Fig. 12. Current flow (i_{s_N}) through the six dc strings—nonisolated L.P.S.

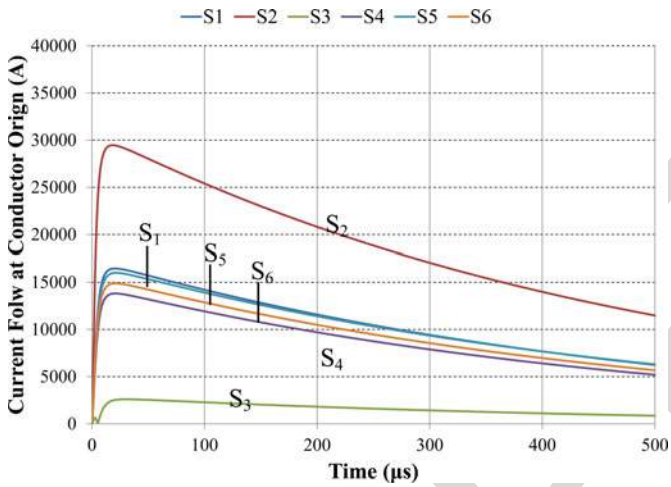

Fig. 13. Current flow (i_{s_N}) through the six dc strings—isolated L.P.S.

B. Time-Domain Simulation Results

Fig. 12 illustrates the calculated time-domain current profiles (i_{s_N}) through the six dc strings considered for the simulation model of Fig. 9 (nonisolated L.P.S), when the lightning current is injected at location A.

Fig. 13 illustrates the calculated current profiles (i_{s_N}) through the six dc strings for the isolated L.P.S design illustrated by Fig. 11, when the lightning strikes also at location A. It is reiterated that the same PV park dimensions (see Fig. 5) and lightning current 150 kA 10/350 μs are considered in both models.

A thorough investigation of Figs. 12 and 13 reveals that the magnitude of the lightning current flow through the six dc strings depends on the type of the external L.P.S employed (isolated or nonisolated). For example, in the nonisolated L.P.S case study, the peak transient current calculated (S_2) is at 37.5 kA, whereas the peak transient current for the isolated case is 29.5 kA, under the same field topology and lightning current energization condition.

In the nonisolated L.P.S system (see Fig. 9), the lightning current divides across all the metallic parts of the PV base, which are common with the external L.P.S. However, in the isolated L.P.S, the lightning current uses only the isolated rod to discharge the current in the earthing system. In this case, it may be that some current will return to the structural bases through the common earthing system.

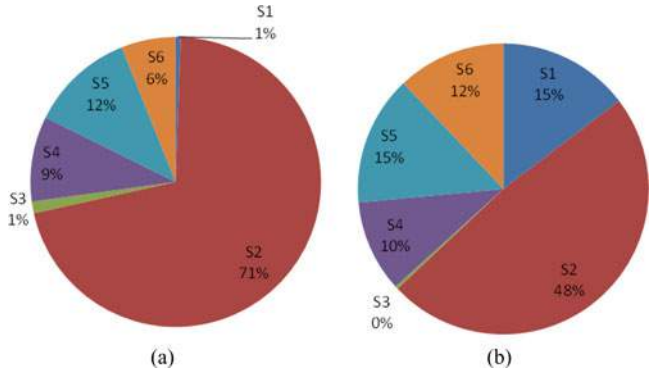

Fig. 14. Energy distribution across a 150-kW solar park (a) Nonisolated L.P.S. (b) Isolated L.P.S.

C. Sensitivity Analysis

The percent lightning current and associated energy distribution across the dc strings modeled can also be assessed through Fig. 14. The assessment reflects on the lightning current injection at location A of Figs. 9 and 11. The associated energy is calculated as follows:

$$E_{s\_N} = \int_0^t i_{s\_n}(t)^2\, dt. \tag{3}$$

The results show that there is a diversified lightning current distribution across the whole area of the park.

Although this diversification would be generally true, it should be emphasized that the distribution of current will depend on: 1) point of lightning strike, 2) dimensions of the park, and 3) the relative positioning of the arrays in the field, as well as on other project specific details (soil resistivity and structure, electrode material used).

It should be noted at this point that the dc side of the inverter should be protected from all possible lightning current routes [2]. According to the European technical specification TS 50539-12, the power surge protective devices associated with PV applications are separated into two categories depending on their discharge current capability. Type 1 (T1) for primary protection against lightning currents I_{imp} (10/350 μs) and Type 2 (T2) for secondary protection against surge currents I_n (8/20 μs).

1) Lightning Current Injection Location: As previously noted, the worst case scenario is expected when the lightning current *i(t)* is injected at location B (see Figs. 9 and 11). This is simply because location B is closer to the array/string combiner box. Table IV tabulates a comparison of the calculated energy (3), for each of the two location scenarios modeled. The results reflect on the maximum lightning current (and associated energy) which is, as expected, from the PV array that has suffered

TABLE IV
CALCULATED ENERGY OF CURRENT WAVEFORMS

	Calculated Energy (kJ)			
	Non- Isolated L.P.S Fig. 9		*Isolated L.P.S Fig.11*	
	Location A	*Location B*	*Location A*	*Location B*
S_2	485.33	819.43	237.5	397.67

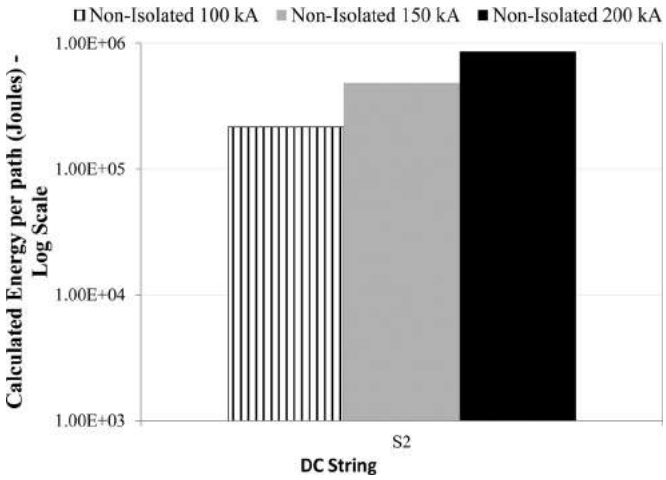

Fig. 15. Maximum dissipated energy across the 150-kW solar park with non-isolated L.P.S for different L.P.Cs.

the lightning strike (S_2), and is worst for the lightning current injected at location B.

2) Lightning Protection Class: One of the features of the simulation models developed is their ability to assess the external L.P.S and earthing system for large-scale solar applications under different pragmatic conditions and scenarios. Thus, the maximum dissipated energy of the S_2 dc strings (see Figs. 9 and 11, respectively) may also be calculated in accordance to the L.P.Cs I (200 kA), II (150 kA), and III and IV (100 kA). The assessment has been applied both in the nonisolated and isolated designs. It is noted that the energy dissipated is shown only for the S_2 dc string, bearing in mind that 1) lightning can strike anywhere and 2) the same design is used throughout the park occupying area. This scenario (S_2 dc string) is sufficient for comparison since it provides the highest stress that would be generated by the lightning strike.

Fig. 15 shows the dissipated energy across the 150-kW solar park with nonisolated L.P.S for the L.P.Cs (I, II, III and IV). The results are illustrated on a log scale. Similarly, Fig. 16 illustrates the dissipated energy calculated for the system having an isolated L.P.S under the requirements dictated by the three L.P.Cs.

3) Effect of Modifying the Earthing Design: A further set of sensitivity analysis demonstrates the effect of enhancing the earthing system of the PV park. Fig. 17 illustrates a modified version of the simulation model illustrated in Fig. 9—i.e., when the lightning strikes at location *A*. In this model, the earthing system is reinforced by adding three additional earth Cu electrodes (7 m each) having a CSA of 50 mm^2.

Fig. 18 illustrates the percent change in the energy dissipated on the S_2 dc string, when benchmarking the two simulation models of Figs. 9 and 17. It is obvious that the maximum energy

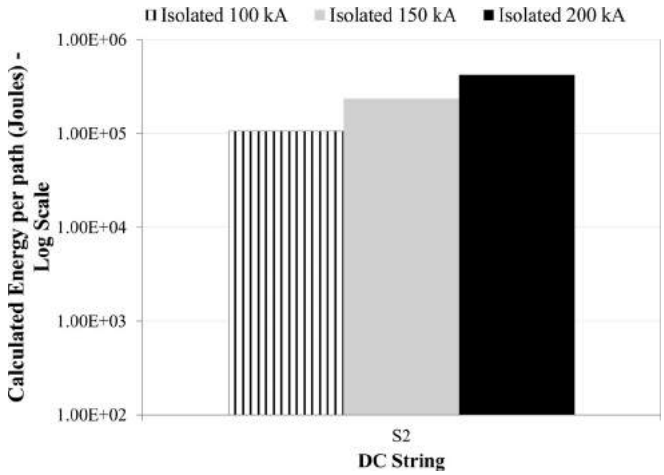

Fig. 16. Maximum dissipated energy across the 150-kW solar park with non-isolated L.P.S for different L.P.Cs.

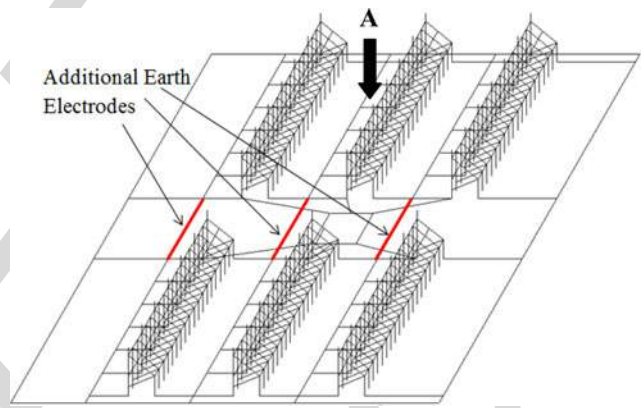

Fig. 17. Real-scale simulation model for a 150-kW solar park—with nonisolated L.P.S and additional earth electrodes to enhance the earthing system.

would be dissipated on the system is significantly reduced. In fact, a total of 75% energy dissipation reduction is calculated under the earthing system arrangement proposed in Fig. 18.

4) Effect of Altering Soil Resistivity: A final set of sensitivity analysis illustrates the effect, (see Fig. 19) of alterating the soil resistivity from a uniform 100 Ω.m to a uniform 1000 and 10 Ω.m soil environments, respectively. This analysis particularly considers the maximum dissipated energy across the 150-kW solar park under the nonisolated L.P.S simulation model (see Fig. 9).

The sensitivity analysis has shown that there is a small change in the maximum energy dissipated across the dc strings. This is due to the fact that the earthing system is common across the uniform soil environment which surrounds the entire PV plant. Therefore, even by altering soil resistivity, the current sharing in the PV metal, and wiring parts will show a small change. In the software used, lightning is an ideal current source and will force the current to discharge even through high resistances. However, a significant influence of soil resistivity would be observed in nonuniform soil models [15] (e.g., two-layer vertical model), i.e., by assuming that the PV farm is occupying different soil layers. In such a case, the lightning current flowing into a

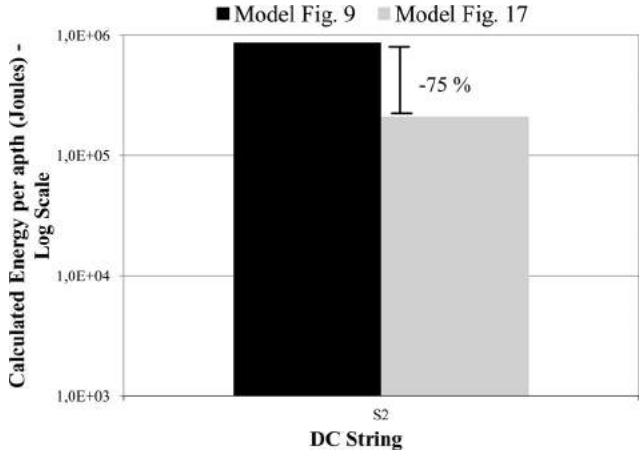

Fig. 18. Comparison of maximum energy dissipation under different earthing system designs.

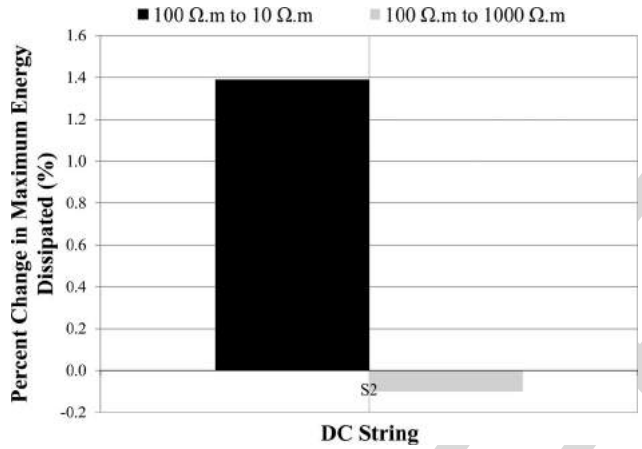

Fig. 19. Comparison of maximum energy dissipation under different soil resistivity values.

lower resistivity soil layer will increase with respect to a higher resistivity soil layer.

V. Conclusion

This paper has provided information and introduced geometrically accurate models to assess the L.P.S and earthing designs in large-scale solar applications. The protection of such large-scale systems is not yet covered by any industrial standards. Therefore, this paper can be used as a starting point for engineers to turn their design endeavors toward calibrated L.P.S and earthing designs for large-scale solar applications. It is demonstrated that the dc strings leading to the inverter should be protected, irrespective of the type of the external L.P.S employed (isolated or nonisolated). This should be done in accordance to the L.P.Cs I, II, and III and IV as dictated by a preceding risk assessment. Furthermore, it is shown that the use of additional earth electrodes to enhance the earthing system of the PV system reduces the energy dissipated. This will in turn reduce the need to oversize the surge protection equipment.

Finally, it is noted that the contents of this paper are general in the sense that they provide information that conform with the requirements of installing external L.P.Ss in large-scale solar field applications.

References

[1] *Low-voltage surge protective devices surge protective devices for specific application including d.c. Part 11 requirements and tests for SPDs in photovoltaic applications*, CENELEC PREN 50539-11-2010.
[2] J. C. Hernandez, P. G. Vidal, and F. Jurado, "Lightning and surge protection in photovoltaic installations," *IEEE Trans. Power Del.*, vol. 23, no. 4, pp. 1961–1971, Oct. 2008.
[3] H.-J. Stern and H. C. Karner, "Lightning induced EMC phenomena in photovoltaic modules," in *Proc. IEEE Int. Symp. Electromagn. Compat.*, Aug. 1993, pp. 442–446.
[4] H. Häberlin and R. Minkner, "A simple method for lightning protection of PV-systems," in *Proc. 12th Eur. Photovoltaic Sol. Energy Conf.*, Apr. 1994, pp. 1885–1888.
[5] *Protection Against Lightning Part 1: General Principles. Edition 2.0*, IEC Standard 62305-1, 2010-2012.
[6] *Protection against Lightning – Part 3: Physical Damage to Structures and Life Hazards*, IEC Standard 62305-3, 2006.
[7] *LV Surge Protective Devices – Part 12: Surge Protective Devices Connected to LV Power Distribution Systems – —Selection and Application Principles*, IEC Standard 61643-12, 2002.
[8] N.D. Kokkinos, N. Christofides, and C.A. Charalambous, "Lightning protection practice for large-extended photovoltaic installations," in *Proc. Int. Conf. Lightning Protection*, Sep. 2–7, 2012, pp. 1–5.
[9] A. Selby and F. Dawalibi, "Determination of current distribution in energized conductors for the computation of electromagnetic fields," *IEEE Trans. Power Del.*, vol. 9, no. 2, pp. 1069–1078, Apr. 1994.
[10] *Protection against lightning—Part 2: Risk management*, Edition 2.0, IEC 62305-2, 2010-12.
[11] *Lightning protection components (LPC). Requirements for connection components*, IEC 50164-1, Sep. 2008.
[12] *Lightning Protection Components (LPC) - Part 2: Requirements for conductors and earth electrodes*, IEC 50164-2, Sep. 2008.
[13] F. P. Dawalibi and A. Selby, "Electromagnetic fields of energized conductors," *IEEE Trans. Power Del.*, vol. 8, no. 3, pp. 1275–1284, Jul. 1993.
[14] *IEEE Guide for Safety in AC Substation Grounding*, IEEE Standard 80-2000.
[15] F. P. Dawalibi, J. Ma, and R. D. Southey, "Behaviour of grounding systems in multilayer soils: a parametric analysis," *IEEE Trans. Power Del.*, vol. 9, no. 1, pp. 334–342, Jan. 1994.
[16] *Protection against lightning—Part 3: Physical Damage to Structure and Life Hazard 2.0*, IEC 62305-3, 2010–12.

Charalambos A. Charalambous (M'05) received the Class I B.Eng. (Hons.) degree in electrical and electronic engineering in 2002, and the Ph.D. degree in electrical power engineering from the University of Manchester Institute of Science and Technology, Manchester, U.K., in 2005.

He is currently an Assistant Professor in the Department of Electrical and Computer Engineering, University of Cyprus, Nicosia, Cyprus. His research interests include dc-induced corrosion, ferroresonance and risk assessment, and management of power systems.

Nikolaos D. Kokkinos received the M.Sc. and Ph.D. degrees in high-voltage engineering from the University of Manchester Institute of Science and Technology, in 2001 and 2004, respectively.

He is currently the Technical Manager of the Research and Development Department of ELEMKO SA, Athens, Greece. Since 2007, he has been an active member as an expert in 1) the International standardization committee IEC SC 37 A, 2) the European standardization committee CLC TC 37, and 3) the European standardization committee CLC SC 9XC.

Nicholas Christofides received the B.Eng. degree in electronics and electrical engineering from Birmingham University, Birmingham, U.K., and the M.Sc. and Ph.D. degrees in electrical engineering from the University of Manchester Institute of Science and Technology, Manchester, U.K.

He is currently with the Department of Electrical Engineering, Frederick University, Nicosia, Cyprus. His research interests include renewable energy sources and especially photovoltaics studying issues such as power quality, lightning protection, and ageing.

External Lightning Protection and Grounding in Large-Scale Photovoltaic Applications

Charalambos A. Charalambous, *Member, IEEE*, Nikolaos D. Kokkinos, and Nikolas Christofides

***Abstract*—The development of large-scale photovoltaic (PV) plants in rural areas is constantly increasing. However, the knowledge of performing and installing lightning and surge protection in large-scale PV plants is still premature. The main objective of this paper is to provide a method for assessing the external lightning protection and earthing designs that may be installed in large-scale solar applications. Consequently, the method and models presented in this paper may assist engineers to perform a comparison between the use of isolated and nonisolated lightning protection systems, and second to select suitable surge protection equipment.**

***Index Terms*—Earthing, large-scale PV plants, lightning protection.**

I. Introduction

THE installation of an efficient lightning protection system (L.P.S) for large-scale photovoltaic (PV) plants is important by virtue of its preventing nature. Primarily, this importance lies in preventing any physical damage to structures as well as life hazards.

Furthermore, it should be borne in mind that the capital investments for large-scale PV plants are significant and the investors should choose to adopt an appropriate L.P.S for their systems. In fact, the cost of installing an L.P.S may be proved insignificant when compared to the revenue losses incurred due to failures or damages resulting from a lightning strike. One should also consider the practical difficulties associated with the repairs or component replacements.

Nevertheless, the knowledge of performing and installing lightning and surge protection in large and extended PV plants with long cabling loops is, in most of the cases, still precipitous. It is worth noting that the recent development of the new CENELEC document of TS 50539-12: 2009 by WG1 of CLC TC37 A [1] only describes the application principles for surge protection in PV installations on roofs of domestic structures.

Moreover, a thorough literature survey reveals that there is still very little information published regarding the design of lightning and surge protection for large-scale solar applications. In particular, the work described in [2] comprehensively covers the related scientific background of any previous work [3], [4] and further emphasizes the lack of 1) specific field experience and 2) a universal standard method to address the problems. To this extent, the current practice, for protecting small-scale PV installations from lightning surges, rests with adopting (partly) protective measures described in standards for conventional low-voltage power distribution systems [5]–[7]. On a relevant note, the work in [8] describes a scaled down laboratory test to investigate the performance of nonisolated and isolated external L.P.S designs in controlling the induced voltages across the dc cable loop of the string due to a lightning strike.

The simulation models formulated in this paper are based on topologically accurate 3-D designs and on other material particulars found in real-life applications. It should be noted that the topologically accurate models include the earthing system arrangement and the metallic PV supporting frames simulated under different scenarios. These models were designed and processed within a commercial software platform utilizing methods described in [9]. The models can be used to assess the design options and the lightning current distribution across large-scale PV parks. Thus, the main objective of this paper is to assess the external lightning protection and earthing design options that are installed in these applications. On a final note, this paper does not account for any induced voltages and currents into the PV arrays that are subject to related lightning channels and flows of the return strokes.

II. Fundamental Design Principles of External L.P.S and Earthing Systems for Large-Scale PV Systems

The design options considered in lightning protection endeavors should be subject to an appropriate risk assessment. The risk assessment may be performed according to IEC-62305-2 [10], which provides a procedure for the evaluation of risk (based on different types of loss) to a structure, due to lightning flashes to earth. For example, in large-scale PV applications, the economic losses may be the dominating factor that determines which type of surge protection should be employed. It is emphasized, however, that this paper takes a step forward and focuses on the design principles of an external L.P.S and earthing systems of the large-scale PV systems. These protection systems are assumed to be the product of appropriate risk assessments.

The L.P.S first embraces the air termination system, which intercepts between the lightning and the physical parts of the protected structure. Second, it embraces the down conductors which discharge the lightning current to an earth termination

Manuscript received May 24, 2013; revised June 25, 2013 and August 22, 2013; accepted August 26, 2013.

C. A. Charalambous is with the Department of Electrical and Computer Engineering, University of Cyprus, Nicosia 1687, Cyprus (e-mail: cchara@ucy.ac.cy).

N. D. Kokkinos is with ELEMKO SA, 144 52 Athens, Greece (e-mail: n.kokkinos@elemko.gr).

N. Christofides is with the Department of Electrical Engineering, Frederick University, Nicosia 1036, Cyprus (e-mail: n.christofides@frederick.ac.cy).

Color versions of one or more of the figures in this paper are available online at http://ieeexplore.ieee.org.

Digital Object Identifier 10.1109/TEMC.2013.2280027

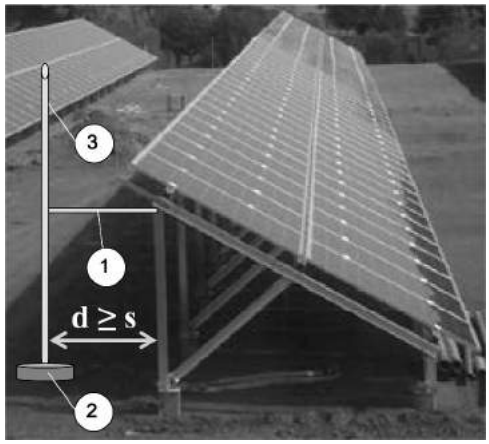

Fig. 1. Isolated L.P.S in PV applications. (1) Isolating support. (2) Concrete block base. (3) Air termination rod.

system. The earth termination system discharges the lightning current into the general mass of the earth.

A. Design Principles of External L.P.S

The main design methods of air termination systems in solar applications are the protection angle or the rolling sphere method. The protection angle method assumes a number of air termination rods with sufficient height, installed along the entire length of the PV supporting infrastructure. These will offer a protection angle which fulfills the required protection set by the L.P.S class [5]. In contrast, when the rolling sphere method is applied, the positioning of the air termination system should ensure that no point of the supporting infrastructure is in contact with a sphere of radius R. To this extent, the external L.P.S can be designed to be isolated or nonisolated from the PV application. The isolated L.P.S is commonly used in cases of high risk damage from the lightning current (should this pass through the metallic installations that are directly connected to the L.P.S). An isolated L.P.S consists of a free standing mast (embracing the air termination rod and the down conductor), which stands away from the PV metallic support frame at a distance d (see Fig. 1).

The separation distance d should always be greater or equal to a minimum separation distance s calculated as follows:

$$s = \frac{k_i}{k_m} \times k_c \times l \tag{1}$$

where k_i is a constant that depends on the selected class of the L.P.S, k_m is a constant that depends on the electrical insulation material, k_c is a constant that depends on the (partial) lightning current flowing in the air termination and the down conductor, and l is the length, in meters, along the air termination and the down conductor [6]. Distance l spans from the top level of the PV supporting infrastructure to the nearest equipotential bonding point or the earth termination system (i.e., ground level).

An example of a nonisolated L.P.S is shown in Fig. 2. This is directly installed on the PV frame provided that the metallic façade/frame can be utilized as a natural component of the L.P.S. However, in such a case, there are certain requirements that need

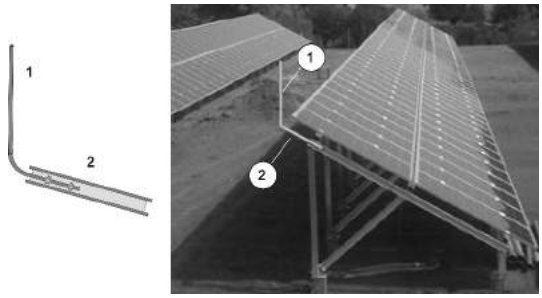

Fig. 2. Nonisolated L.P.S in PV applications. (1) Aluminum air termination rod. (2) Connection clamp.

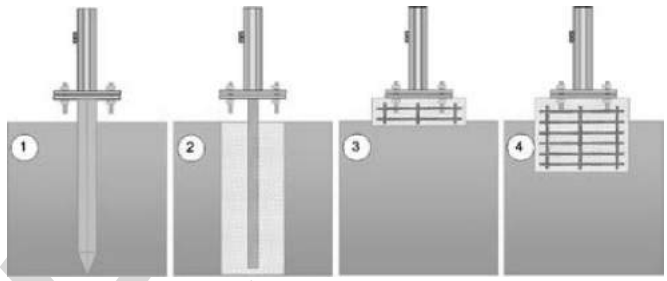

Fig. 3. Type of foundation for an earthing system of the open-field PV applications.

TABLE I
TYPE OF FOUNDATION AND MATERIALS FOR AN EARTHING SYSTEM

	Type of Foundation	Material for Earthing System Driven into the Soil
1	Galvanized steel directly buried into the soil	Galvanized steel, Stainless steel
2	Steel profile embedded in concrete	Copper coated steel, Copper, Stainless steel
3	Reinforced concrete block placed above ground level	Galvanized steel, Copper coated steel, Copper, Stainless steel
4	Reinforced concrete foundation into the soil	Copper coated steel, Copper, Stainless steel
Note 1: Copper Conductor may be tinned; Note 2: Aluminum not allowed to be buried into the soil		

to be fulfilled as per the clause 5.3.4 of IEC/EN 62305-3. These requirements are summarized as follows: 1) the dimensions of the metallic façade should conform the requirements of EN 50164-1&2 [11], [12] and future IEC 62561-2, and 2) the connections along the metallic façade length shall be secure by such means as brazing, welding, clamping, crimping, screwing, or bolding.

B. Design Principles of Earthing Systems

A primary objective in designing the earthing system of a large-scale PV application is to maintain a balance between the installation cost as well as the efficiency and lifetime of the system. Consequently, an important parameter that the designer should take into account when selecting the earth electrode material is the foundation type employed in PV façade framework. That is to avoid the galvanic corrosion between metals of dissimilar nature. Thus, all the materials used (i.e., earth rods, bonding conductors, metallic façade, clamps) should be homogeneous. Fig. 3 illustrates the most common types of PV framework foundations and Table I tabulates their description and the associated material characteristics of the earthing system driven into the

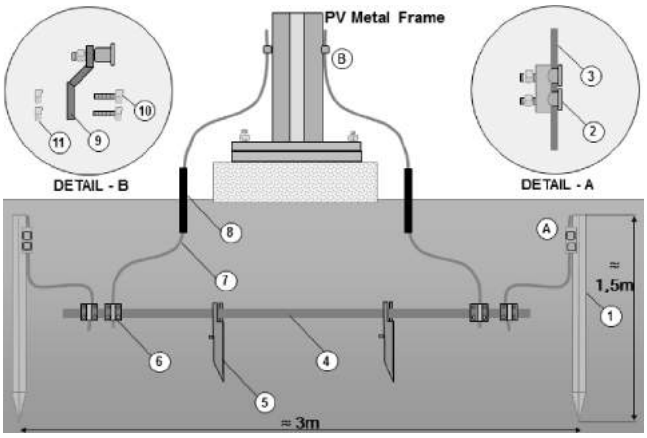

Fig. 4. Application example of type A earth electrode of hot dip galvanized material in combination with dip driven galvanized steel profiles or reinforced concrete blocks.

TABLE II
DESCRIPTION OF THE ELEMENTS ON TYPE A APPLICATION EXAMPLE

	Description
1	Hot dip galvanized steel (St/tZn) earth rod cross profile with zinc coating of 500 g/m^2 (~70 μm coating thickness), 1.5 m long tested as per EN 50164 -2
2	Hot dip galvanized steel double bonding clamp between St/Zn 10 mm round conductor and St/Zn cross profile earth rod tested as per EN 50164 1 (Type H 100 kA)
3	Hot dip galvanized steel round conductor 10 mm diameter with zinc coating of 50 μm long tested as per EN 50164 -2
4	Hot dip galvanized steel strip conductor with dimensions 30mm x 3mm zinc coating of 500 g/m^2 (~70 μm coating thickness), tested as per EN 50164 -2
5	Hot dip galvanized steel strip conductor fastener for vertical installation of the strip conductor.
6	Hot dip galvanized steel clamp St/tZn 10mm round conductor and St/tZn 30mm wide strip conductor tested as per EN 50164 -1 (Type H – 100kA)
7	Hot dip galvanized steel round conductor 10mm diameter with zinc coating of 50 μm tested as per EN 50164-2.
8	Corrosion protection PVC insulation tape
9	Aluminium (Al) end clamp between metallic (St/tZn or Al) surface and St/tZn 10 mm round conductor tested as per EN 50164 1 (Type H -100 kA)
10,11	2 x stainless steel or hot dip galvanized (St/tZn) M8 screw and nut

soil, to avoid galvanic corrosion, thus extending the life time of the installation.

Furthermore, the large area that the solar field applications occupy suggests the combined use of type A and type B earthing systems [16]. The most common type A electrodes, utilized in large-scale solar applications, are the earth rods which are vertically installed into the soil. The field experience suggests that at least two rods should be used per down conductor as illustrated in Fig. 4 having a minimum length of 1.5 m. Furthermore, it is also important to maintain a distance between the earth rods installed $\sim$2 times their length. Table II tabulates the elements and material characteristics of Fig. 4.

For type B earth electrodes, the most common shape used is the strip conductor. The use of type B electrodes ensures the equipotential bonding of all PV metal frameworks. Fig. 5 illustrates an application of a type B earth electrode in an open-field solar application. A common mesh size spans on a $20m \times 20m$ basis, although wider mesh sizes such as $40m \times 40m$ may also be utilized when combined with type A electrodes.

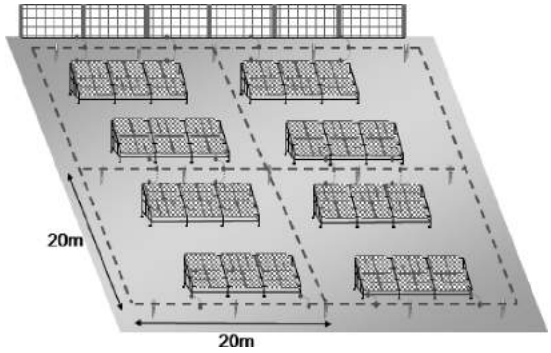

Fig. 5. Application of type B earth electrode in an open-field PV application.

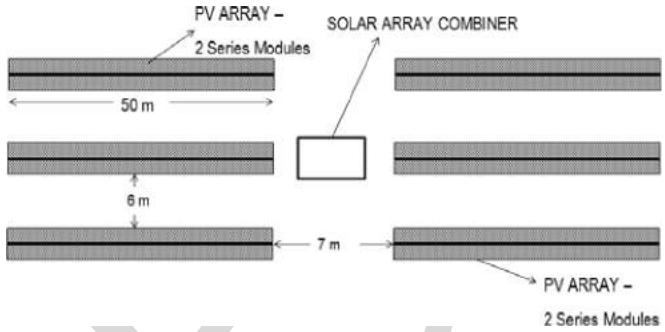

Fig. 6. Topology of the 150-kWp PV system.

III. DESCRIPTION OF THE SIMULATION MODELS

The real-scale simulation models were formulated within a commercially available software by following an assessment of the infrastructure elements considered to contribute to the lightning performance of both isolated and nonisolated L.P.S installed on large-scale solar applications. The software employs a Cartesian coordinate system with three coordinates (x, y, z), thus allowing the formation of topologically accurate simulation models, through the use of conductors. The arrangement of conductors is specified by virtue of its energization method, the magnitude of the energization, its material coating characteristics, and the coordinates of each conductor along with its radii and number of specified segments. The conductors segments can be subsequently associated with various energization types (potentials, current injections, and current flows) [9], [13].

A. Description of the System

The system considered consists of 600 250 Wp modules, directly linked to the MV network, with a nominal output power of 150 kWp, occupying an area of 1605 m^2. Six similar structures (arrays) of fixed inclination are considered and each structure holds up to 100 modules as is shown in Fig. 6. The length of each PV array is 50 m and two rows of PV modules are assumed to be installed on each structure.

Furthermore, Fig. 7 illustrates an earthing design example when a non isolated L.P.S is installed in the solar field applications. It specifically shows two rows of PV arrays (6 m away) that are connected to a common earth electrode via the metallic framework.

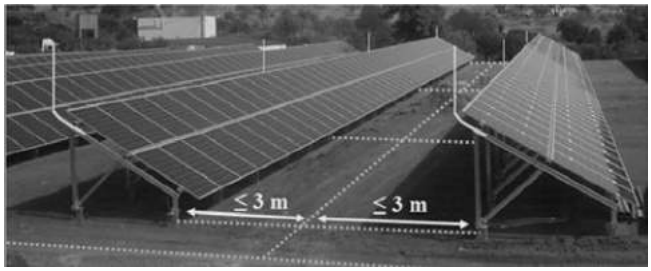

Fig. 7. Example of nonisolated L.P.S and earthing design for large-scale solar field applications.

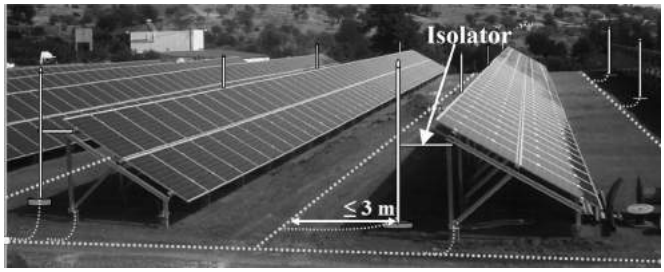

Fig. 8. Example of isolated L.P.S and earthing design for large-scale solar field applications.

Alternatively, Fig. 8 illustrates an application of an isolated L.P.S and its associated earthing design. It shows that the isolated air termination rods are connected directly to a circumference earth electrode; thus, each row of air termination rods have its own earth electrode. It should be noted that in the case of isolated L.P.S, the earthing system should be designed in such a way to prohibit the circulation of any lightning current through the PV frame.

B. Description of the Simulation Model

Two real-scale simulation models are developed within the software's modules for the 150 kWp PV fixed inclination system of Fig. 6. Following the dimensions given in Fig. 6 and an external L.P.S design similar to Fig. 7, the ideal computer model formulated, for a nonisolated external lightning protection application, is illustrated in side view in Fig. 9.

Fig. 10 also illustrates the design dimensions considered for the PV structural base modeled in the simulation model—to facilitate the fixed inclination of the array structures.

Table III tabulates the further particulars of the numbered items of the conductive elements employed in the computer model (see Fig. 9).

Moreover, (to limit the overall number of conductors used in the model), only one array/string combiner, that may accommodate 150 250 Wp modules, is modeled. As is shown in Fig. 9, a total of six strings (S_1–S_6) lead to the inverter and each string consists of 25 modules in series. In fact, the six strings terminate into the array/string combiner box and from then on to the inverter. The latter simplifies the dc wiring considerably as no overlapping will be necessary between structures and the wiring is kept at its minimum.

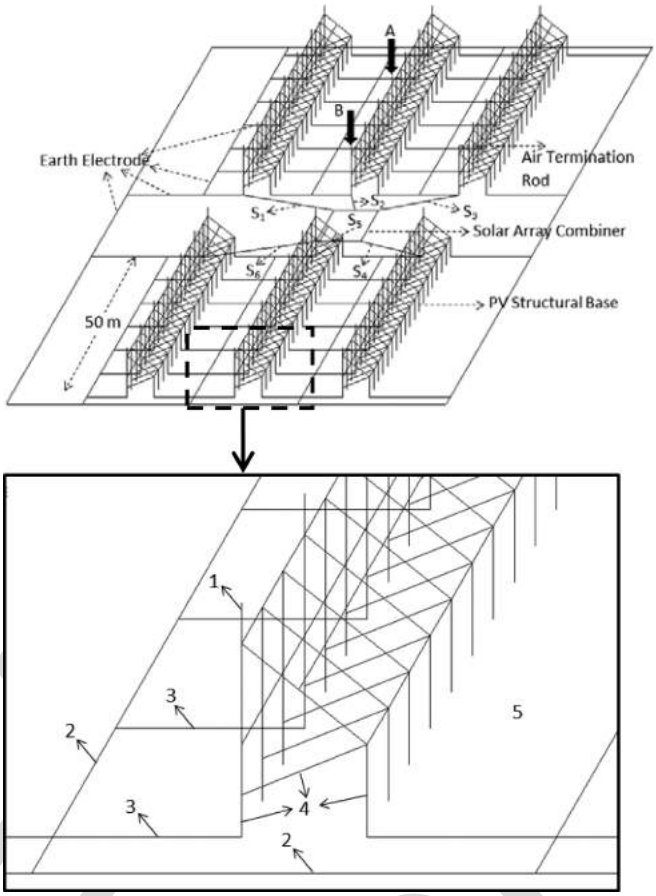

Fig. 9. Real-scale simulation model for a 150-kW solar park—with nonisolated L.P.S.

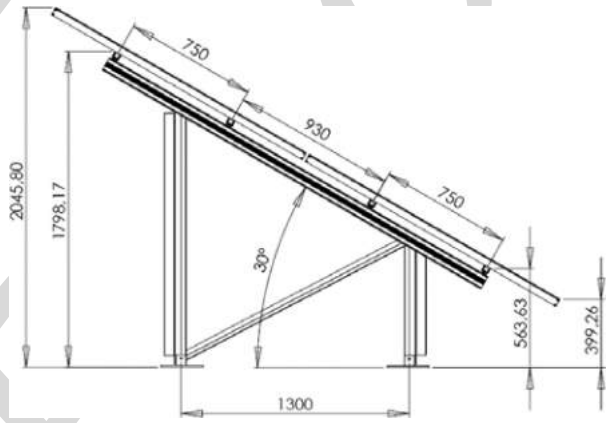

Fig. 10. Design dimensions (mm) of the PV structural base —side view.

Fig. 11 illustrates the ideal simulation model formulated for the same PV application and design characteristics shown in Fig. 6 having, however, an isolated external L.P.S design as illustrated in Fig. 8. In this model (see Fig. 11), the lightning rod (item 1_A) is isolated from the PV structural base. More specifically, this is an aluminum air termination rod, Φ16 mm, 3 m long, located 0.5 m away from the structural base, and is attached to a circumference earth electrode as shown in Fig. 11. The further particulars of the numbered items of the conductive

TABLE III
DESCRIPTION OF THE CONDUCTIVE ELEMENTS OF THE SIMULATION MODEL

Numbered Items	Further Particulars
Attached Lightning Rod (Item 1)	Aluminium air termination rod, Φ16mm, 1m long, attached on the PV support structure. Designed as per Class I L.P.S [5] Number of Lightning Rods*: 7 Spacing*: ~7m *Evaluated as per IEC 62305-3 [16] (rolling sphere method)
Earth Electrodes (Items 2 & 3)	Earth electrodes are made of copper conductors (CSA 50mm^2) buried into soil at a depth of 0.5m. The structural PV base is bonded (item 3) to the circumference earth electrode (item 2) to ensure an equipotential continuity.
Structural Base (Item 4)	Geometrically accurate aluminium support PV structure as per the dimensions given in Fig 10. Each metallic component of the base is approximated by 10mm radius aluminium conductors. The vertical conductors (legs) of the structure are driven to a depth of 1.5m into the earth.
Soil (Item 5)	The soil resistivity is assumed to be 100 Ω.m.

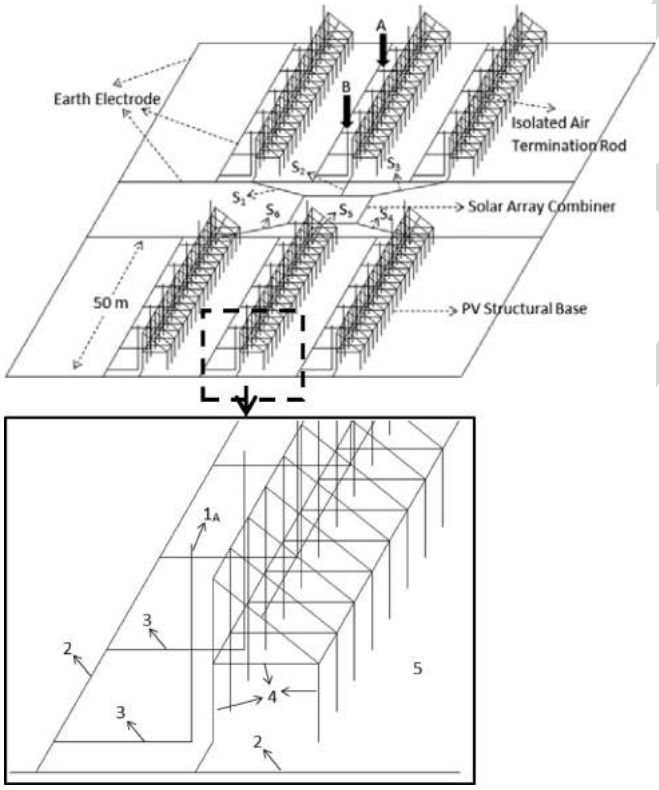

Fig. 11. Real-scale simulation model for a 150-kW solar park—with isolated L.P.S.

elements employed in this computer model are the same as those tabulated in Table III.

Finally, two possible locations (A or B) for lightning current injections are assumed in this paper, for both the simulation models shown in Figs. 9 and 11. These locations are arbitrary chosen, however, location B may be considered as a worst case scenario as it is closer to the array/string combiner box. It is noted that the model is able to account for any other lightning injection location specified by the user. The lightning surge currents considered in this paper are defined by double exponential type functions. A lightning surge current *I(t),* can be injected at the specified location (A or B) as illustrated by Figs. 9 and 11. The current is classified as 150 kA 10/350 μs, to account for a lightning protection class (L.P.C) II as per IEC 62305-1. The corresponding double exponential function considered is given as follows:

$$I(t) = 153664 \times 10^3 \cdot \left[e^{-a \cdot t} - e^{-\beta \cdot t}\right] \tag{2}$$

where $\alpha = 2049$ and $\beta = 563758$.

On a final note, the 150-kWp PV plant, considered previously is assumed to be directly connected to the LV or the MV grid via a transformer (e.g., installed on wooden poles). It should be noted that for PV plants of higher power level, a high-voltage substation may be required [14]. However, the lack of specific standards calls for further research to justify different earthing design methods that balance cost and safety. For example, a 4-MW PV park may occupy a field area that equals to 90000 m^2. A uniform mesh size grid (as used in ac substations) across the field may be prohibitively expensive at this scale; however, safety should not be compromised.

IV. SIMULATION RESULTS AND ANALYSIS

The ultimate objective of the simulations is to assess the lightning current distribution across a large-scale PV park, under the two different external L.P.S design options (isolated or non-isolated). The simulations are carried out using the two models illustrated in Figs. 9 and 11, respectively. This exercise is particularly important as it may facilitate an appropriate specification (discharge current capability) of the surge arrester devices entitled to protect the inverter, based on the topology and type of protection of each individual solar application.

A. Reference to Computational Methods

The software computes the current distribution for the networks modeled (see Figs. 9 and 11) consisting both the aerial and buried conductors excited at selected frequencies, determined by the type of lightning current considered. The details of the evaluation method are given in [9] and [13].

The time-domain responses are obtained as follows. The double exponential 150-kA function (2) is decomposed into its frequency spectrum, by a forward fast Fourier transform. For the 150-kA double exponential function considered (2), computations are carried out for selected frequencies ranging from 0–1 MHz. At selected frequencies, the electromagnetic fields are calculated at various observation points, on the conductor network, to obtain the frequency spectrum of the electromagnetic fields. The time-domain transient current profiles, through each conductor (or observation point) of the system, are subsequently calculated by appropriately superimposing the frequency domain responses obtained.

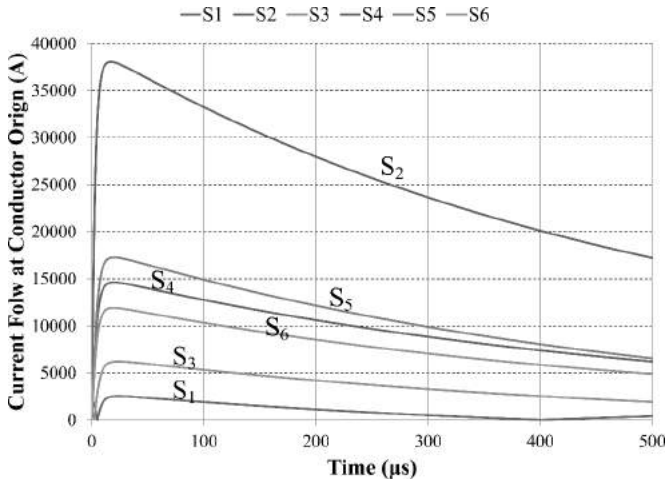

Fig. 12. Current flow (i_{s_N}) through the six dc strings—nonisolated L.P.S.

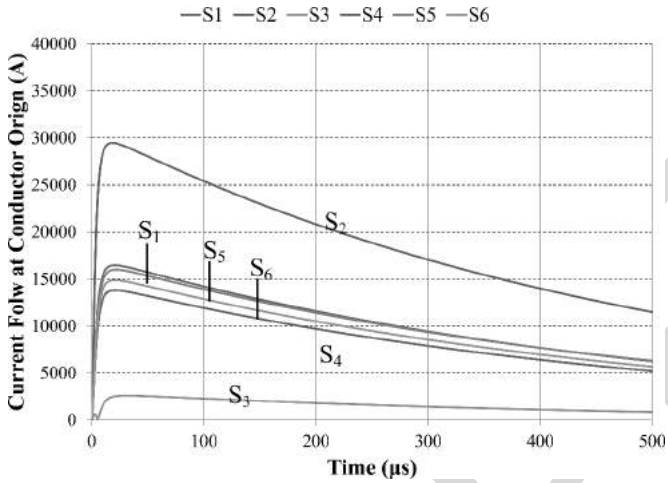

Fig. 13. Current flow (i_{s_N}) through the six dc strings—isolated L.P.S.

B. Time-Domain Simulation Results

Fig. 12 illustrates the calculated time-domain current profiles (i_{s_N}) through the six dc strings considered for the simulation model of Fig. 9 (nonisolated L.P.S), when the lightning current is injected at location A.

Fig. 13 illustrates the calculated current profiles (i_{s_N}) through the six dc strings for the isolated L.P.S design illustrated by Fig. 11, when the lightning strikes also at location A. It is reiterated that the same PV park dimensions (see Fig. 5) and lightning current 150 kA 10/350 μs are considered in both models.

A thorough investigation of Figs. 12 and 13 reveals that the magnitude of the lightning current flow through the six dc strings depends on the type of the external L.P.S employed (isolated or nonisolated). For example, in the nonisolated L.P.S case study, the peak transient current calculated (S_2) is at 37.5 kA, whereas the peak transient current for the isolated case is 29.5 kA, under the same field topology and lightning current energization condition.

In the nonisolated L.P.S system (see Fig. 9), the lightning current divides across all the metallic parts of the PV base, which are common with the external L.P.S. However, in the isolated L.P.S, the lightning current uses only the isolated rod to discharge the current in the earthing system. In this case, it may be that some current will return to the structural bases through the common earthing system.

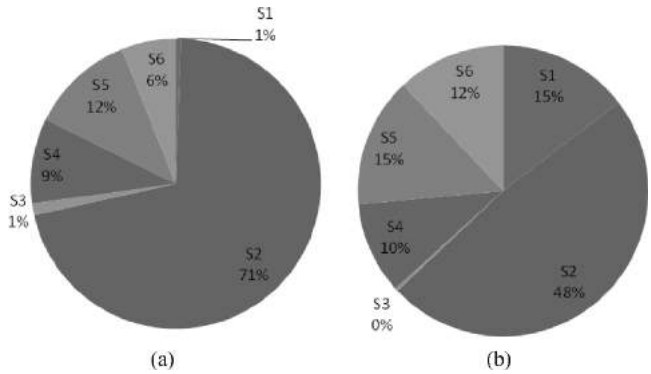

Fig. 14. Energy distribution across a 150-kW solar park (a) Nonisolated L.P.S. (b) Isolated L.P.S.

C. Sensitivity Analysis

The percent lightning current and associated energy distribution across the dc strings modeled can also be assessed through Fig. 14. The assessment reflects on the lightning current injection at location A of Figs. 9 and 11. The associated energy is calculated as follows:

$$E_{s\_N} = \int_0^t i_{s\_n}(t)^2\, dt. \tag{3}$$

The results show that there is a diversified lightning current distribution across the whole area of the park.

Although this diversification would be generally true, it should be emphasized that the distribution of current will depend on: 1) point of lightning strike, 2) dimensions of the park, and 3) the relative positioning of the arrays in the field, as well as on other project specific details (soil resistivity and structure, electrode material used).

It should be noted at this point that the dc side of the inverter should be protected from all possible lightning current routes [2]. According to the European technical specification TS 50539-12, the power surge protective devices associated with PV applications are separated into two categories depending on their discharge current capability. Type 1 (T1) for primary protection against lightning currents I_{imp} (10/350 μs) and Type 2 (T2) for secondary protection against surge currents I_n (8/20 μs).

1) Lightning Current Injection Location: As previously noted, the worst case scenario is expected when the lightning current *i(t)* is injected at location B (see Figs. 9 and 11). This is simply because location B is closer to the array/string combiner box. Table IV tabulates a comparison of the calculated energy (3), for each of the two location scenarios modeled. The results reflect on the maximum lightning current (and associated energy) which is, as expected, from the PV array that has suffered

TABLE IV
CALCULATED ENERGY OF CURRENT WAVEFORMS

	Calculated Energy (kJ)			
	Non- Isolated L.P.S Fig. 9		*Isolated L.P.S Fig.11*	
	Location A	*Location B*	*Location A*	*Location B*
S_2	485.33	819.43	237.5	397.67

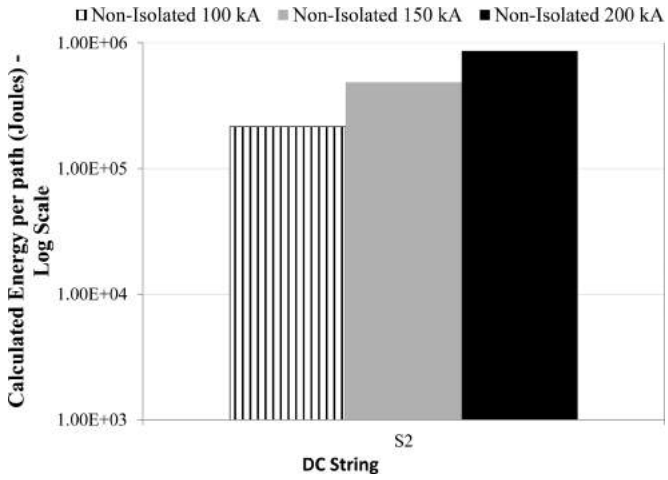

Fig. 15. Maximum dissipated energy across the 150-kW solar park with non-isolated L.P.S for different L.P.Cs.

the lightning strike (S_2), and is worst for the lightning current injected at location B.

2) Lightning Protection Class: One of the features of the simulation models developed is their ability to assess the external L.P.S and earthing system for large-scale solar applications under different pragmatic conditions and scenarios. Thus, the maximum dissipated energy of the S_2 dc strings (see Figs. 9 and 11, respectively) may also be calculated in accordance to the L.P.Cs I (200 kA), II (150 kA), and III and IV (100 kA). The assessment has been applied both in the nonisolated and isolated designs. It is noted that the energy dissipated is shown only for the S_2 dc string, bearing in mind that 1) lightning can strike anywhere and 2) the same design is used throughout the park occupying area. This scenario (S_2 dc string) is sufficient for comparison since it provides the highest stress that would be generated by the lightning strike.

Fig. 15 shows the dissipated energy across the 150-kW solar park with nonisolated L.P.S for the L.P.Cs (I, II, III and IV). The results are illustrated on a log scale. Similarly, Fig. 16 illustrates the dissipated energy calculated for the system having an isolated L.P.S under the requirements dictated by the three L.P.Cs.

3) Effect of Modifying the Earthing Design: A further set of sensitivity analysis demonstrates the effect of enhancing the earthing system of the PV park. Fig. 17 illustrates a modified version of the simulation model illustrated in Fig. 9—i.e., when the lightning strikes at location *A*. In this model, the earthing system is reinforced by adding three additional earth Cu electrodes (7 m each) having a CSA of 50 mm^2.

Fig. 18 illustrates the percent change in the energy dissipated on the S_2 dc string, when benchmarking the two simulation models of Figs. 9 and 17. It is obvious that the maximum energy

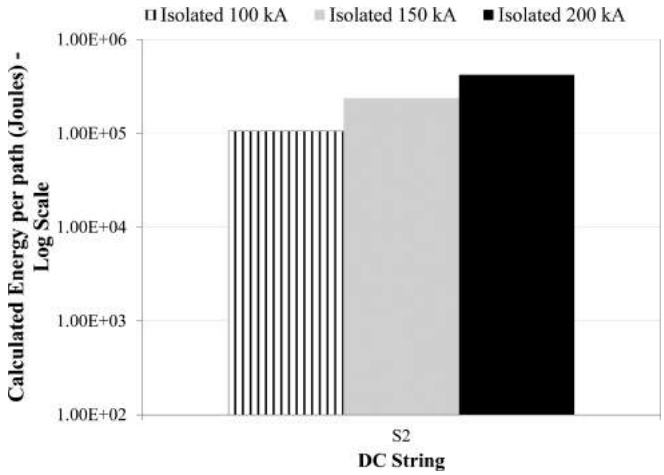

Fig. 16. Maximum dissipated energy across the 150-kW solar park with non-isolated L.P.S for different L.P.Cs.

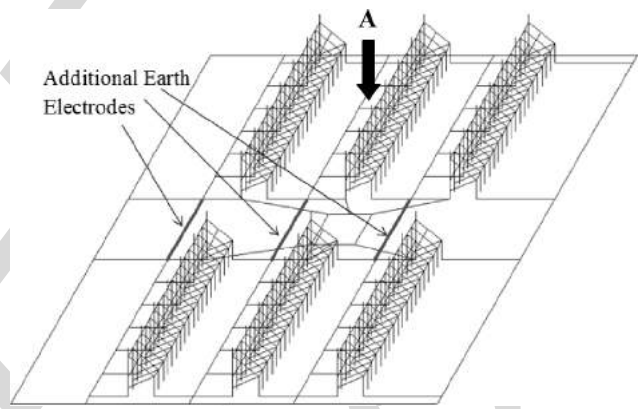

Fig. 17. Real-scale simulation model for a 150-kW solar park—with nonisolated L.P.S and additional earth electrodes to enhance the earthing system.

would be dissipated on the system is significantly reduced. In fact, a total of 75% energy dissipation reduction is calculated under the earthing system arrangement proposed in Fig. 18.

4) Effect of Altering Soil Resistivity: A final set of sensitivity analysis illustrates the effect, (see Fig. 19) of alterating the soil resistivity from a uniform 100 Ω.m to a uniform 1000 and 10 Ω.m soil environments, respectively. This analysis particularly considers the maximum dissipated energy across the 150-kW solar park under the nonisolated L.P.S simulation model (see Fig. 9).

The sensitivity analysis has shown that there is a small change in the maximum energy dissipated across the dc strings. This is due to the fact that the earthing system is common across the uniform soil environment which surrounds the entire PV plant. Therefore, even by altering soil resistivity, the current sharing in the PV metal, and wiring parts will show a small change. In the software used, lightning is an ideal current source and will force the current to discharge even through high resistances. However, a significant influence of soil resistivity would be observed in nonuniform soil models [15] (e.g., two-layer vertical model), i.e., by assuming that the PV farm is occupying different soil layers. In such a case, the lightning current flowing into a

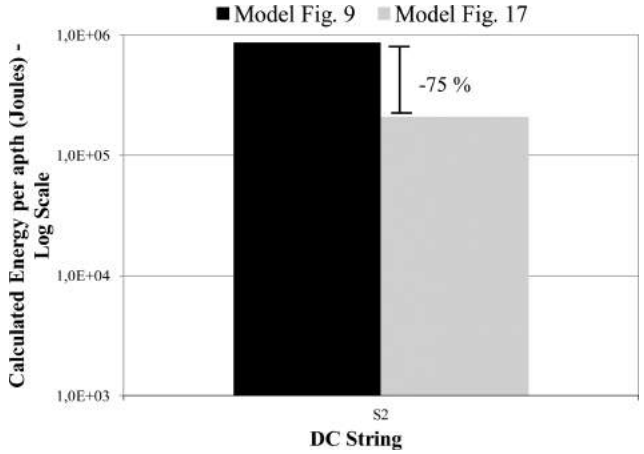

Fig. 18. Comparison of maximum energy dissipation under different earthing system designs.

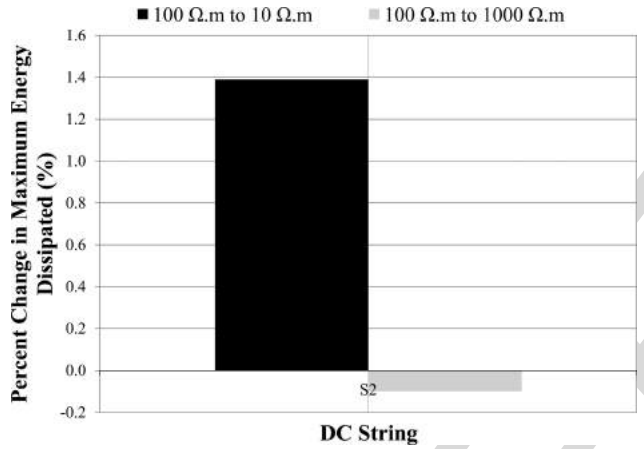

Fig. 19. Comparison of maximum energy dissipation under different soil resistivity values.

lower resistivity soil layer will increase with respect to a higher resistivity soil layer.

V. Conclusion

This paper has provided information and introduced geometrically accurate models to assess the L.P.S and earthing designs in large-scale solar applications. The protection of such large-scale systems is not yet covered by any industrial standards. Therefore, this paper can be used as a starting point for engineers to turn their design endeavors toward calibrated L.P.S and earthing designs for large-scale solar applications. It is demonstrated that the dc strings leading to the inverter should be protected, irrespective of the type of the external L.P.S employed (isolated or nonisolated). This should be done in accordance to the L.P.Cs I, II, and III and IV as dictated by a preceding risk assessment. Furthermore, it is shown that the use of additional earth electrodes to enhance the earthing system of the PV system reduces the energy dissipated. This will in turn reduce the need to oversize the surge protection equipment.

Finally, it is noted that the contents of this paper are general in the sense that they provide information that conform with the requirements of installing external L.P.Ss in large-scale solar field applications.

References

[1] *Low-voltage surge protective devices surge protective devices for specific application including d.c. Part 11 requirements and tests for SPDs in photovoltaic applications*, CENELEC PREN 50539-11-2010.
[2] J. C. Hernandez, P. G. Vidal, and F. Jurado, "Lightning and surge protection in photovoltaic installations," *IEEE Trans. Power Del.*, vol. 23, no. 4, pp. 1961–1971, Oct. 2008.
[3] H.-J. Stern and H. C. Karner, "Lightning induced EMC phenomena in photovoltaic modules," in *Proc. IEEE Int. Symp. Electromagn. Compat.*, Aug. 1993, pp. 442–446.
[4] H. Häberlin and R. Minkner, "A simple method for lightning protection of PV-systems," in *Proc. 12th Eur. Photovoltaic Sol. Energy Conf.*, Apr. 1994, pp. 1885–1888.
[5] *Protection Against Lightning Part 1: General Principles. Edition 2.0*, IEC Standard 62305-1, 2010-2012.
[6] *Protection against Lightning – Part 3: Physical Damage to Structures and Life Hazards*, IEC Standard 62305-3, 2006.
[7] *LV Surge Protective Devices – Part 12: Surge Protective Devices Connected to LV Power Distribution Systems – —Selection and Application Principles*, IEC Standard 61643-12, 2002.
[8] N.D. Kokkinos, N. Christofides, and C.A. Charalambous, "Lightning protection practice for large-extended photovoltaic installations," in *Proc. Int. Conf. Lightning Protection*, Sep. 2–7, 2012, pp. 1–5.
[9] A. Selby and F. Dawalibi, "Determination of current distribution in energized conductors for the computation of electromagnetic fields," *IEEE Trans. Power Del.*, vol. 9, no. 2, pp. 1069–1078, Apr. 1994.
[10] *Protection against lightning—Part 2: Risk management*, Edition 2.0, IEC 62305-2, 2010-12.
[11] *Lightning protection components (LPC). Requirements for connection components*, IEC 50164-1, Sep. 2008.
[12] *Lightning Protection Components (LPC) - Part 2: Requirements for conductors and earth electrodes*, IEC 50164-2, Sep. 2008.
[13] F. P. Dawalibi and A. Selby, "Electromagnetic fields of energized conductors," *IEEE Trans. Power Del.*, vol. 8, no. 3, pp. 1275–1284, Jul. 1993.
[14] *IEEE Guide for Safety in AC Substation Grounding*, IEEE Standard 80-2000.
[15] F. P. Dawalibi, J. Ma, and R. D. Southey, "Behaviour of grounding systems in multilayer soils: a parametric analysis," *IEEE Trans. Power Del.*, vol. 9, no. 1, pp. 334–342, Jan. 1994.
[16] *Protection against lightning—Part 3: Physical Damage to Structure and Life Hazard 2.0*, IEC 62305-3, 2010–12.

Charalambos A. Charalambous (M'05) received the Class I B.Eng. (Hons.) degree in electrical and electronic engineering in 2002, and the Ph.D. degree in electrical power engineering from the University of Manchester Institute of Science and Technology, Manchester, U.K., in 2005.

He is currently an Assistant Professor in the Department of Electrical and Computer Engineering, University of Cyprus, Nicosia, Cyprus. His research interests include dc-induced corrosion, ferroresonance and risk assessment, and management of power systems.

Nikolaos D. Kokkinos received the M.Sc. and Ph.D. degrees in high-voltage engineering from the University of Manchester Institute of Science and Technology, in 2001 and 2004, respectively.

He is currently the Technical Manager of the Research and Development Department of ELEMKO SA, Athens, Greece. Since 2007, he has been an active member as an expert in 1) the International standardization committee IEC SC 37 A, 2) the European standardization committee CLC TC 37, and 3) the European standardization committee CLC SC 9XC.

Nicholas Christofides received the B.Eng. degree in electronics and electrical engineering from Birmingham University, Birmingham, U.K., and the M.Sc. and Ph.D. degrees in electrical engineering from the University of Manchester Institute of Science and Technology, Manchester, U.K.

He is currently with the Department of Electrical Engineering, Frederick University, Nicosia, Cyprus. His research interests include renewable energy sources and especially photovoltaics studying issues such as power quality, lightning protection, and ageing.